Available online at www.sciencedirect.com

ScienceDirect

IFAC Papers Online CONFERENCE PAPER ARCHIVE

IFAC-PapersOnLine 49-23 (2016) 089–096

A control framework for biologically inspired underwater swimming manipulators equipped with thrusters ⋆

J. Sverdrup-Thygeson * **E. Kelasidi** * **K. Y. Pettersen** * **J. T. Gravdahl** **

* *Centre for Autonomous Marine Operations and Systems, Department of Engineering Cybernetics, NTNU, Norwegian University of Science and Technology, Trondheim, Norway, (e-mail: {Jorgen.Sverdrup-Thygeson, Eleni.Kelasidi, Kristin.Y.Pettersen}@itk.ntnu.no)*

** *Department of Engineering Cybernetics, NTNU, Norwegian University of Science and Technology, Trondheim, Norway, (e-mail: Tommy.Gravdahl@itk.ntnu.no)*

Abstract: In this paper we present a control framework for a novel biologically inspired underwater swimming manipulator (USM) equipped with thrusters. The framework consists of a kinematic part and a dynamic part. The kinematic part of the framework controls the velocity of the head link of the USM by coordinating the motion of the body of the USM and the articulated joints. Various methods based on inverse kinematics is presented and the applicability of each method for kinematic control of the USM is discussed. The dynamic part of the framework ensures that the velocity references generated by the inverse kinematics method are followed and that the thruster forces are appropriately distributed among the available thrusters. The significance of the relationship between the inverse kinematics routine and the thruster allocation algorithm is explained and simulations are included to validate the concept for control of the USM.

Keywords: Underwater Swimming Manipulator (USM), inverse kinematic control of USM, thruster allocation for USM

1. INTRODUCTION

More and more oil and gas installations and operations are performed subsea, and the need for services such as installation support and subsea inspection, maintenance, and repair (IMR) are increasing. Until recently, subsea supporting services have mainly been performed using remotely operated vehicles (ROVs) equipped with one or more manipulator arms (Marani et al., 2009), also referred to as underwater vehicle manipulator systems (UVMS) (Fossen, 1991; Schjølberg and Fossen, 1994).

Traditional ROVs are large and heavy, expensive to operate, and they require constant supervision. The time to mobilize and deploy them is also quite long. Consequently, the industry has recognized the need for less costly, small, lightweight, and autonomous units that can perform routine inspection tasks at subsea oil and gas installations and even carry out light intervention (Gilmour et al., 2012). In particular, there has been an increasing interest for developing AUVs with hovering capabilities, precise maneuverability, and ability to operate in confined areas. AUVs equipped with robotic arms, so-called intervention AUVs (I-AUVs) (Ridao et al., 2014), are also experiencing increased attention. The dexterity of these manipulator equipped AUVs are however quite crude.

The generic underwater swimming manipulator (USM) presented in Sverdrup-Thygeson et al. (2016) has the potential to overcome the challenges mentioned for ROVs/AUVs. A USM is a crossover between a typical ROV/AUV and an underwater snake robot (USR) (see Figure 1). It is a hyper-redundant mechanism with the ability to perform its own locomotion and serve as a robot manipulator at the same time. With its slender and articulated body, the USM is able to access even the narrow parts of a subsea installation, areas which have previously been inaccessible due to the size of most ROVs/AUVs. In this paper, we study a specific type of USM equipped with a stern propeller and several tunnel thrusters along the body of the USM.

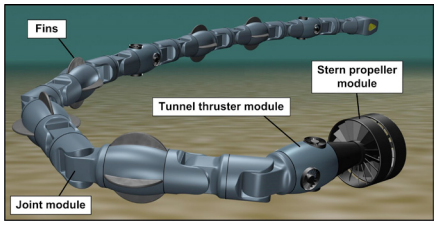

Fig. 1. Underwater swimming manipulator

Underwater snake robots without thrusters achieve locomotion by emulating motion patterns inspired by the motion of its biological siblings. Adding thruster modules to an articulated mechanism like this is a novel approach that opens up for a whole new range of application areas for underwater snake robots. The tail thruster induces linear forces along the body which increase the overall velocity of the robot. Maneuverability can be greatly improved, since a USM with thrusters can achieve forward velocity and even vertical and sideways motion without performing undulatory motion. We consider

⋆ This research was partly funded by the Research Council of Norway through the Centres of Excellence funding scheme, project No. 223254 NTNU AMOS, and partly funded by VISTA, a basic research program in collaboration between The Norwegian Academy of Science and Letters, and Statoil.

2405-8963
Peer review under responsibility of International Federation of Automatic Control.
10.1016/j.ifacol.2016.10.326

this as a great advantage, especially when operating in narrow spaces where the undulating motion would otherwise be severely constrained. The ability to perform linear displacements along the body can also improve the collision avoidance capabilities. Finally, the USM is able to hover under water at a fixed location enabling the USM to act as a manipulator arm in order to perform stationary inspection or light intervention tasks. The flexibility of this hyper-redundant manipulator arm will provide a dexterity that exceeds the manipulator arms of ROVs/AUVs today. Other biologically inspired robots, such as underwater snake robots and robotic fish, do not yet possess the same hovering capabilities as the USM, and thus they are not as well suited for inspection and intervention operations as the USM.

In order to realize operational USMs for underwater inspection and intervention tasks, several control problems needs to be addressed. One of the primary goals is to make the USM end-effector (i.e. the head link) follow a desired task space trajectory. This can be achieved by dynamic control (Fossen, 1991; Schjølberg and Fossen, 1994). However, Antonelli (2014) suggests that kinematic control is the preferred choice due to uncertainties in the hydrodynamic parameters and the possibility to exploit the kinematic redundancy of the system. For a USM, utilizing the redundancy means coordinating the motion of the USM as a rigid body and the motion of the articulated joints, while considering various performance criteria.

Coordination between the motion of the USM as a rigid body and the motion of the articulated joints can be solved in a number of different ways. Egeland (1987) employs a macro-micro approach for distributing motion between a slow gross positioning part and a faster manipulator part. In Yamamoto and Yun (1992) motion coordination is achieved by making a specific reference point on the mobile platform follow a trajectory calculated algebraically by the manipulability index of the 2-link non-redundant manipulator. Another approach for ground-based mobile robots are presented in Pham and From (2013), where a virtual mass-damper-spring system is inserted between the mobile base and the end-effector. Kinematic control of a UVMS using the task priority approach is presented in e.g. Antonelli and Chiaverini (1998). Siciliano and Slotine (1991) generalizes the task priority approach to multiple tasks and presents case studies with highly redundant snake-like robots. Kinematic control of a ground-based snake robot with non-holonomic constraints is reported in Matsuno and Suenaga (2003). For a UVMS, various performance criteria have been investigated in terms of optimal motion coordination, in e.g. Sarkar and Podder (2001); Han et al. (2011); Mohan et al. (2012). Redundancy resolution with multiple tasks is also reported in Antonelli and Chiaverini (2003); Soylu et al. (2010) using fuzzy logic, and in Casalino et al. (2012) using dynamic programming. The combination of an adaptive dynamic controller and an inverse kinematic algorithm for controlling a UVMS is studied in Sarkar et al. (1999). To the authors' best knowledge, none of these techniques have been applied for motion coordination of USMs with thrusters.

In this paper, we present a complete framework for the control of a USM. The proposed framework consists of a kinematic part and a dynamic part. We discuss the applicability of kinematic control for the USM and present three commonly used methods and how these can be applied for motion coordination. The kinematic part of the system employs first-order inverse kinematics to generate reference velocity signals for the joints

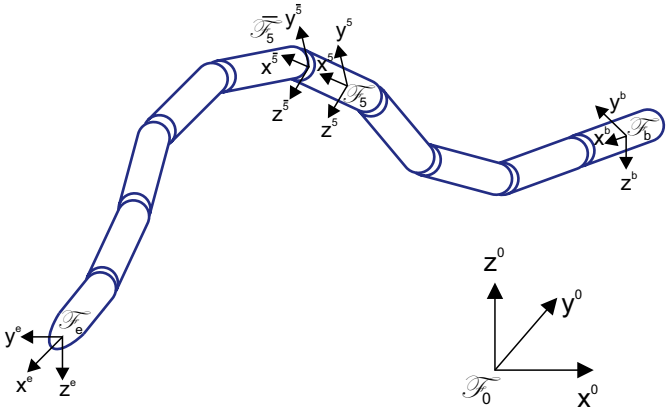

Fig. 2. Reference frames

and for the USM as a rigid body. A dynamic controller calculates generalized forces and moments, which are then optimally distributed among the thrusters using a thruster allocation algorithm. Finally, we perform simulations using the model from Sverdrup-Thygeson et al. (2016) to validate the proposed framework for control of the USM.

The paper is organized as follows. In Section 2 we present a generic framework for control of a USM and discuss the different subsystems. The kinematics of the end-effector of the USM expressed in the body-fixed end-effector frame is derived in Section 3, and various methods for inverse kinematic control suitable for a USM are presented in Section 4. Section 5 discusses the challenges associated with the design of a configuration space dynamic controller and how to distribute the thruster forces. Finally, simulation results and conclusions are presented in Sections 6 and 7.

2. FRAMEWORK FOR CONTROL OF A USM WITH THRUSTERS

In this section we introduce the overall framework intended for motion control of the USM. We present two different operating modes and discuss the responsibilities of the different subsystems of the framework.

The USM is considered as a free-floating serial chain robot manipulator consisting of n rigid links, connected by $n-1$ motorized joints. The USM is moving fully submerged and is equipped with p thrusters; one tail thruster and $p-1$ thrusters distributed along the body of the USM. Link 1 is referred to as the tail link and link n is referred to as the head link.

Figure 2 illustrates the different reference frames. The reference frame $\mathscr{F}_0$ is defined and referred to as the inertial frame. The base frame $\mathscr{F}_b$ is a body-fixed frame with its origin fixed at the center of mass of the tail link and axes coinciding with the longitudinal, transversal, and normal axes of the link. Likewise, frame $\mathscr{F}_i$ is attached to the center of mass of link i with axes specified in the same way as for the base frame. The reference frame $\bar{\mathscr{F}}_i$ is located at the center of joint i and the axes of rotation are parallel to the axes of frame $\mathscr{F}_i$. Finally, the frame $\mathscr{F}_e$ is the end-effector frame with its origin fixed in the head link, e.g. inside a gripper tool or coinciding with the position and orientation of a built-in camera.

Figure 3 shows an illustration of the subsystems of the proposed framework. This partitioning is similar to typical guidance, controller, and allocation frameworks for underwater and surface

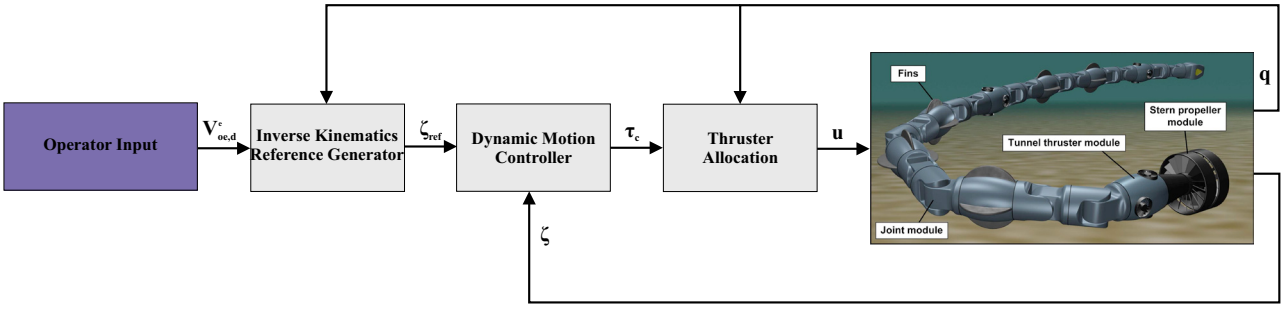

Fig. 3. Control framework for the USM

vessels. However, the subsystems for the USM face additional challenges due to the time-varying configuration of the USM. The main responsibilities of the subsystems are:

- *Inverse kinematics reference generator* - calculates the reference joint velocities and the reference linear and angular velocity of the base frame.
- *Dynamic motion controller* - determines the required generalized forces and moments to be applied to the USM in order to follow the reference velocity of the base frame and the required joint torques to achieve tracking of the joint velocity reference signals.
- *Thruster allocation* - distributes the control efforts among the available thrusters in an optimal manner.
- *Underwater swimming manipulator* - physical model of the USM.

In Figure 3, the desired end-effector velocity, $\mathbf{V}^e_{0e,d}$, is one of several possible inputs from the operator controlling the USM. In this paper, we consider an operator specifying the desired velocity of the head link based on the video feed from a camera attached to the head link.

The USM as a free-floating robot manipulator arm with added thrusters has more control inputs than required to fulfill a generic 6 DoF position/orientation task. The USM is thus considered kinematically redundant with respect to this task. Kinematically, the thrusters contribute to the motion of the whole USM as a rigid body, decoupled from the motion of the manipulator arm. However, the number of independent thruster inputs is configuration dependent, since the orientation of the thrusters depend on the joint angles.

A UVMS with fixed thrusters is usually designed such that the vehicle body is fully actuated and thus the end-effector Jacobian of the whole vehicle manipulator system has always full row rank, i.e. the 6 DoF end-effector task can always be kinematically achieved. For a USM, the thruster configuration matrix depends on the joint angles and may loose rank for certain joint configurations. This means that the thrusters will not be able to produce motion in all directions, similar to underwater vehicles that are underactuated by design. However, the USM will still be kinematically redundant as long as the total number of independent control inputs is higher than the dimension of the end-effector task.

In this paper, we propose two operating modes for two different scenarios:

- *Transport mode* - for moving over larger distances to reach a specific area of interest.
- *Work mode* - for low-speed maneuvering while performing an inspection or intervention task.

These two operation modes are further described in the following sections.

2.1 Transport mode

In transport mode the primary goal is to move the USM from the current position to a new position some distance away, while maintaining the desired heading. Obstacles may block the path and collision avoidance along the whole body of the USM is required. If information about the location of the obstacles are available a priori, then the trajectory planner can take this into account. However, in many cases the USM will be moving in an unstructured and unknown environment. Real-time identification of obstacles and solution of the collision avoidance problem are therefore necessary. Moving in confined areas and through narrow openings add further complexity to this problem.

Preliminary results for the transport mode are presented in Sverdrup-Thygeson et al. (2016). In particular, a simple unconstrained solution to the path following problem for a USM with additional effectors is proposed. In Sverdrup-Thygeson et al. (2016) the USM follows a defined path and desired heading using additional effectors for propulsion, rather than using an undulating motion pattern. The effector forces are distributed according to

$$\mathbf{f}_p = \mathbf{T}_W^\dagger \tau_{CM,d} \tag{1}$$

where $\mathbf{T}_W^\dagger = \mathbf{W}^{-1}\mathbf{T}(\psi)^T(\mathbf{T}(\psi)\mathbf{W}^{-1}\mathbf{T}(\psi)^T)^{-1}$ is the generalized inverse, $\mathbf{W}$ is a matrix specifying the relative weighting between the additional effectors, and $\tau_{CM,d}$ are the desired generalized forces and moments on the CM of the USM. We refer to Sverdrup-Thygeson et al. (2016) for additional details.

2.2 Work mode

The work mode is intended for stationary and low-speed maneuvers, while performing an inspection or intervention task. A camera or intervention tool may be integrated in the head link, and the primary control objective is to attain a desired linear and angular head link velocity by coordinating the overall USM motion and using the joints to change the geometry.

For a non-redundant manipulator arm the Jacobian matrix of the manipulator is square, and the angular velocities of the manipulator joints can be resolved by computing the Jacobian inverse. For a free-floating redundant manipulator such as a USM, both the 6 DoF motion of the mechanism itself and the kinematic redundancy of the manipulator arm have to be considered. The kinematic redundancy introduce both advantages and added

complexity in terms of distributing the motion between the USM and the manipulator.

In the next section we describe the kinematics of the USM in 3D, and in Section 4 we discuss the motion coordination using various methods for redundancy resolution.

3. KINEMATICS OF THE END-EFFECTOR

In this section, we derive the forward kinematics and the differential kinematics of the USM end-effector. We use a similar notation as in From et al. (2014).

3.1 Forward kinematics

The position and orientation of $\mathscr{F}_b$ with respect to $\mathscr{F}_0$ is given by the homogeneous transformation matrix

$$g_{0b} = \begin{bmatrix} R_{0b} & p_{0b} \\ 0 & 1 \end{bmatrix} \in \mathbb{R}^{4\times 4}, \tag{2}$$

where $R_{0b} \in SO(3)$ is the rotation matrix describing the orientation of the base frame and $p_{0b} \in \mathbb{R}^3$ is the vector from the origin of $\mathscr{F}_0$ to the origin of $\mathscr{F}_b$. Homogeneous transformation matrices can be multiplied to yield composite transformations. Thus, the location and orientation of $\mathscr{F}_i$ can be described by

$$g_{0i} = g_{0b}g_{bi} = \begin{bmatrix} R_{0i} & p_{0i} \\ 0 & 1 \end{bmatrix}. \tag{3}$$

To simplify the analytical expressions for the kinematics of the USM we choose to work with transformations between the joints, i.e. between frames $\bar{\mathscr{F}}_i$ and $\bar{\mathscr{F}}_{i+1}$. The location and orientation of frame $\bar{\mathscr{F}}_i$ can be described by

$$g_{0\bar{i}} = g_{0b}g_{b\bar{1}} \cdots g_{\overline{(i-1)}\bar{i}}. \tag{4}$$

The forward kinematics of the end-effector is then given by

$$g_{0e} = g_{0b}g_{b\bar{1}} \cdots g_{\overline{n-1}e} = \begin{bmatrix} R_{0e} & p_{0e} \\ 0 & 1 \end{bmatrix}. \tag{5}$$

3.2 Differential kinematics

We know how to describe the position and orientation of the reference frames with respect to each other. Next, we want to find how the joint velocities and the velocity of the base frame translates to the velocity of the head link. In general, there are two ways of doing this, the analytical approach, by direct differentiation of the forward kinematics, and the geometric approach. We define the velocity state of the USM as

$$\zeta = \begin{bmatrix} V_{0b}^b \\ \dot{q} \end{bmatrix} \in \mathbb{R}^{6+(n-1)} \tag{6}$$

where $\dot{q} \in \mathbb{R}^{n-1}$ is the vector of joint velocities, $V_{0b}^b = \begin{bmatrix} (v_{0b}^b)^T & (\omega_{0b}^b)^T \end{bmatrix}^T \in \mathbb{R}^6$ is the velocity twist of the USM base frame, and v_{0b}^b and ω_{0b}^b are the linear and angular body-fixed velocities, respectively.

The analytical Jacobian, $J_a(\eta, q)$, represents the relation between the velocity state of the USM, ζ, and the time derivative of the end-effector position and orientation in the inertial frame. This relation can be expressed as

$$\dot{\eta}_{0e} = J_a(\eta, q)\zeta, \tag{7}$$

and the detailed derivation can be found in e.g. Antonelli (2014).

In this paper, we derive the geometric Jacobian, $J_g(q)$, of the head link expressed in the body-fixed end-effector frame $\mathscr{F}_e$, in a similar way as in From et al. (2014). We choose this approach in order to describe the geometric Jacobian as the mapping between the velocity state of the USM and the body-fixed end-effector velocity. By expressing the velocity coordinate vectors in body-fixed reference frames, we avoid the representation singularity associated with representing orientations using Euler angles.

The end-effector velocity with respect to the inertial frame can be written as the sum of the velocity of the base frame and the velocity of the end-effector relative to the base frame, taking care to represent the velocities in the same reference frame. The end-effector velocity is now expressed in frame $\mathscr{F}_e$ by

$$V_{0e}^e = Ad_{g_{be}}^{-1} V_{0b}^b + V_{be}^e, \tag{8}$$

where $Ad_{g_{be}}$ is the Adjoint map of the transformation matrix g_{be}, and V_{be}^e is the velocity of the end-effector with respect to the base frame. The Adjoint map of a generic transformation matrix g and its inverse is given as (From et al., 2014)

$$Ad_g = \begin{bmatrix} R & \hat{p}R \\ 0 & R \end{bmatrix}, \quad Ad_g^{-1} = \begin{bmatrix} R^T & -R^T\hat{p} \\ 0 & R^T \end{bmatrix}, \tag{9}$$

where the $\hat{}$ operator transforms the corresponding vector into a skew-symmetric matrix.

Since the USM has 1-DoF Euclidean joints, we find the velocity of the end-effector relative to the base frame by adding the contributions of each joint. Using the common Denavit-Hartenberg convention, where all the rotations occur around the local z axis, the manipulator Jacobian, J_m, is defined in the end-effector frame $\mathscr{F}_e$ by

$$V_{be}^e = J_m(q)\dot{q}, \tag{10}$$

where

$$J_m(q) = \begin{bmatrix} z_{\bar{1}} \times p_{\bar{1},e} & z_{\bar{2}} \times p_{\bar{2},e} & \cdots & z_{\overline{n-1}} \times p_{\overline{n-1},e} \\ z_{\bar{1}} & z_{\bar{2}} & \cdots & z_{\overline{n-1}} \end{bmatrix}. \tag{11}$$

We can also express (11) using the Adjoint maps as

$$J_m(q) = \begin{bmatrix} Ad_{g_{\bar{1}e}}^{-1} X_1^1 & Ad_{g_{\bar{2}e}}^{-1} X_2^2 & \cdots & Ad_{g_{\overline{n-1}e}}^{-1} X_{n-1}^{n-1} \end{bmatrix}, \tag{12}$$

where $X_i^i = [0,0,0,0,0,1]^T$ is the body velocity twist of the rotation around the z axis of frame $\bar{\mathscr{F}}_i$.

Finally, we find the geometric Jacobian for the whole USM by inserting (10) in (8)

$$\begin{aligned} V_{0e}^e &= \begin{bmatrix} Ad_{g_{be}}^{-1} & J_m(q) \end{bmatrix} \begin{bmatrix} V_{0b}^b \\ \dot{q} \end{bmatrix} \\ &= J_g(q)\zeta. \end{aligned} \tag{13}$$

Various methods to invert (13) and resolve the velocity state vector ζ are presented next.

4. INVERSE KINEMATIC CONTROL

In this section we present the concept of inverse kinematic control for a USM. We discuss how to fulfill the end-effector

control objectives by combining the motion of the USM as a rigid body with the manipulator motion using the motorized joints.

As explained before, the USM is considered kinematically redundant with respect to the 6 DoF end-effector velocity task. This redundancy can be exploited by introducing secondary objectives to be fulfilled simultaneously with the primary task. We conjecture that the most important secondary control objectives for underwater swimming manipulators, in prioritized order, are to:

- satisfy the mechanical constraints, e.g. maximum joint deflections and maximum angular velocity for the joints
- maintain good manipulability, i.e. avoid singular joint configurations
- maintain controllability, i.e. avoid singular thruster configurations
- avoid collision with other moving objects and stationary obstacles
- minimize the total thruster effort
- minimize drag forces, i.e. attempt to align the USM with the dominant direction of the ocean currents

The reasoning for this is that first of all it is important not to exceed the physical limitations of the articulated structure, as this may break the mechanical joints or subject the structure to extensive wear and tear. Second, it is necessary to maintain good manipulability and controllability to be able to perform maneuvers in narrow spaces and to quickly avoid obstacles detected while moving in a dynamic environment. Third, we want to minimize the thruster effort in order to reduce the power consumption. Finally, it is important to align the USM with the direction of the ocean current such that the fluid drag forces are minimized, as this is related to the energy consumption of the thrusters.

In this paper, we consider the achievement of a specified end-effector velocity expressed in the end-effector frame as the primary control objective. The end-effector velocity is completely specified by the base frame velocity and the joint velocities. The position and orientation of the end-effector will be investigated in future work.

There are some important differences between a USM and a UVMS when it comes to kinematic control:

- The USM can utilize all available degrees of freedom. There is no need to restrict the overall motion of the USM base in order to conserve power, which is often the case for a UVMS due to the large size of the vehicle.
- Avoidance of representation singularities are more important for a USM. The pitch angle of a UVMS is usually restricted, while this is not the case for a USM.
- For a UVMS, the position and orientation of the thrusters are usually fixed with respect to the body-fixed frame. The position and orientation of the built-in thrusters of the USM with respect to the base frame are configuration dependent, i.e. it depends on the joint angles.

In the following, we present different methods to distribute the desired end-effector motion between the USM base frame and the motorized joints, and discuss advantages and disadvantages of each method. All the methods take a desired head link velocity as input and calculates the base frame and joint velocity reference signals.

4.1 Pseudo-inverse

The pseudo-inverse solution is characterized by

$$\zeta_{ref} = J_g^{\dagger}(q) V_{0e,d}^{e}, \tag{14}$$

where $J_g^{\dagger} = J_g^T (J_g J_g^T)^{-1}$. The base frame and the joint velocity reference vector, ζ_{ref}, is resolved using the minimum-norm solution minimizing the base frame and the joint velocities in a least-squares sense. The advantage of this solution is that it utilizes all available control inputs to fulfill the control objective. It is also a simple solution, and therefore it is well suited for initial simulations and concept verification. The main disadvantage is that the base frame will be moving all the time, causing high thruster utilization, potentially increased drag effects, and induced torques in the joints due to the dynamic coupling between the motion of the USM and the joint motion.

4.2 Weighted pseudo-inverse

The weighted pseudo-inverse solution is characterized by

$$\zeta_{ref} = J_{W_g}^{\dagger}(q) V_{0e,d}^{e}, \tag{15}$$

where $J_{W_g}^{\dagger} = W_g^{-1} J_g^T (J_g W_g^{-1} J_g^T)^{-1}$. The weighting matrix, W_g, is a diagonal matrix where the elements can be used to prioritize the use of certain control inputs. As such, the weighted pseudo-inverse solution can distribute the desired motion of the end-effector between the base frame, i.e. moving the USM as a rigid body, and the manipulator joints, by defining an appropriate weighting matrix, W_g.

4.3 Closed-loop singularity-robust task priority approach

The singularity-robust task priority approach (Chiaverini, 1997) is a null-space based method originating from the well-known task priority method (Maciejewski and Klein, 1985; Nakamura et al., 1987). The main advantage is that multiple tasks can be handled with strict prioritization.

If we consider a primary task to follow an end-effector trajectory and a secondary task to keep the base frame of the USM stationary at a desired position, then we can resolve the configuration space velocities of the USM according to

$$\zeta_{ref} = J_g^{\dagger}(q)(V_{0e,d}^{e} + k_p \tilde{\eta}_{0e}) + (I - J_g^{\dagger}(q) J_g(q)) J_s^{\dagger} (V_{0b,d}^{b} + k_s \tilde{\eta}_{0b}), \tag{16}$$

where $V_{0b,d}^{b}$ is the desired base frame velocity twist, and $\tilde{\eta}_{0e}$ and $\tilde{\eta}_{0b}$ are position error vectors for the end-effector and the base frame, respectively. Furthermore, J_s is the Jacobian of the secondary task, and k_p and k_s are suitably chosen controller gains.

From (16), we see that the configuration space velocities introduced by the secondary task are filtered through the null-space of the primary task Jacobian, and they will therefore create internal joint motions that do not interfere with the primary velocity task. The advantages of this solution is the strict prioritization of the tasks, and thus, more predictability in terms of the fulfillment of each task. Also, with the secondary task of keeping the base frame stationary, there will be less movement of the base frame and less thruster utilization. A disadvantage of this particular choice of primary and secondary tasks, is that

the manipulator arm will move all the way to the edge of the workspace before the base frame starts to move. If the primary task can not be satisfied by moving the manipulator arm alone, then the base frame will start to move.

5. DYNAMIC MOTION CONTROLLER AND THRUSTER ALLOCATION

In this section we give a brief presentation of the dynamic motion controller and the generic force allocation concept presented in Sverdrup-Thygeson et al. (2016). Note that in this paper we adapt the force allocation concept to thruster allocation for USMs with a stern propeller and tunnel thrusters distributed along the body of the USM. In particular, we discuss the relationship between the allocation algorithm and the inverse kinematics algorithm presented in Section 4.

The overall performance of the system is dependent on the ability of the dynamic motion controller and the thruster allocation algorithm to achieve the goal of tracking the reference signals generated by the inverse kinematics subsystem. Tracking errors will result in a deviation from the desired end-effector velocity task. Uncertainties in the hydrodynamic parameters together with time-varying disturbances and dynamic coupling between the motion of the joints and the motion of the base, suggest that the controller should be designed using robust nonlinear control methods. Design and analysis of the nonlinear controller is not within the scope of this paper. Since the primary objective is velocity control of the end-effector and only velocity references are available from the IK routine, we choose in this paper a simple proportional controller for the base frame and joint velocities, expressed by

$$\tau_c = \mathbf{K}_p(\zeta_{ref} - \zeta), \tag{17}$$

where τ_c is the commanded generalized forces and moments to be distributed by the thruster allocation algorithm.

For a generic overactuated system there are many different ways to distribute the control efforts among the effectors and yet obtain the same net forces and moments. Proper force allocation is therefore required to do so in an optimal manner. Control allocation has been studied extensively in the context of motion control for different systems. A recent survey on control allocation methods and applications is given in Johansen and Fossen (2013). A typical control allocation algorithm relies on input from a high-level motion control law producing a vector of virtual inputs, which in many cases is interpreted as the desired generalized forces and moments. The primary objective of the control allocation algorithm is then to distribute commands among the actuators such that the total forces and moments produced equals the desired virtual input (Johansen and Fossen, 2013).

As shown in Sverdrup-Thygeson et al. (2016), we express the total forces and moments exerted by the thrusters in matrix form as

$$\tau = \mathbf{T}(\psi)\mathbf{f}_p, \tag{18}$$

where $\mathbf{T}(\psi)$ is the thruster configuration matrix and $\mathbf{f}_p$ is the vector of scalar thruster forces. The thruster forces are resolved according to

$$\mathbf{f}_p = \mathbf{T}_W^{\dagger}\tau_c, \tag{19}$$

where $\mathbf{T}_W^{\dagger} = \mathbf{W}^{-1}\mathbf{T}(\psi)^T(\mathbf{T}(\psi)\mathbf{W}^{-1}\mathbf{T}(\psi)^T)^{-1}$ is the generalized inverse of $\mathbf{T}(\psi)$.

For the USM, let m be the number of degrees of freedom for the thrusters to control. The USM is equipped with p thrusters, and the thruster configuration matrix $\mathbf{T}(\psi)$ consists of p column vectors, one for each thruster. In this paper, the column vectors define the mappings between the thruster forces and the generalized forces and moments exerted on the USM. This may be forces and moments acting on the center of mass of the USM or any other body-fixed location. The generalized forces and moments should be co-located with the velocity state of the USM.

A major difference between a USM and a surface or underwater vessel in terms of thruster force allocation, is that the latter has fixed thruster positions. This is not the case for a USM. When the geometry of the USM is changed, the relative position and orientation of the thruster with respect to the base frame is also changed, which in turn changes the thruster configuration matrix. The configuration matrix will thus be a function of the joint angles. The rank, r, of the configuration matrix is defined as the number of linearly independent rows of $\mathbf{T}(\psi)$. Due to the variable structure of the USM, $\mathbf{T}(\psi)$ may become rank deficient for certain joint configurations.

For surface vessels with azimuth thrusters, the thruster angles are usually assigned individually to avoid rank deficiency of the configuration matrix, since this is associated with loss of motion capability in one or more directions. In the framework proposed in this paper, the reference joint velocities are resolved using inverse kinematics. The issue of singularity robustness and rank deficiency of the thruster configuration matrix should therefore be handled by the inverse kinematics subsystem.

When $r = m$ there is just enough independent control forces to achieve the desired generalized forces and moments. When $r > m$ the thruster configuration is said to be redundant, and secondary objectives can be included in the thruster allocation algorithm. If the thruster configuration matrix becomes rank deficient, i.e. $r < m$, the matrix $(\mathbf{T}(\psi)\mathbf{W}^{-1}\mathbf{T}(\psi)^T)$ becomes singular and non-invertible. In order to avoid this, we can use a damped least-squares solution. This will, however, cause a deviation from the commanded generalized forces and moments.

In this paper, we therefore make the following simplifying assumption:

Assumption 1. The USM is equipped with enough thrusters to avoid the risk of rank deficiency, i.e. $\mathbf{T}(\psi)$ has always full row rank.

Remark 1. Assumption 1 means that the USM is always fully actuated. The assumption can be relaxed if the inverse kinematics routine is designed to take into account the current rank of the thruster configuration matrix.

Simulation results and validation of the proposed control framework for the USM are presented in the next section.

6. SIMULATION RESULTS

In this section, we validate the proposed control framework for the USM through simulations. We show that the USM is able to achieve the desired end-effector (i.e. head link) velocity.

We consider a USM with $n = 16$ links, each one having length $2l_i = 0.14$ m and mass $m_i = 0.6597$ kg. The simulation model

presented in Sverdrup-Thygeson et al. (2016) is used for the simulations, representing the physical USM operating in a virtual 2D horizontal plane. The simulated USM consists of elliptic link sections with major and minor diameters $2a = 2 \cdot 0.03$ m and $2b = 2 \cdot 0.05$ m, respectively, and it is equipped with $p = 9$ thrusters attached to links 1, 2, 4, 6, 8, 10, 12, 14, and 16. The fluid properties are assumed to be $\rho = 1000$ kg/m^3 and $C_f = 0.03$, $C_D = 2$, $C_A = 1$, $C_M = 1$, and the hydrodynamic related parameters $\mathbf{c}_t$, $\mathbf{c}_n$, $\boldsymbol{\mu}$, $\boldsymbol{\Lambda}_1$, $\boldsymbol{\Lambda}_2$, and $\boldsymbol{\Lambda}_3$ are computed by using equations derived in Kelasidi et al. (2014). The controller gains are selected as $\mathbf{K}_p = \text{diag}(2000, 2000, 1600, 1000, \ldots, 1000) \in \mathbb{R}^{3+(n-1),3+(n-1)}$. The simulations are performed in *Matlab* using the *ode23tb* solver with a relative and absolute error tolerance of 10^{-4}.

The selected end-effector velocity profile for this case study represents motion in a square pattern. For proof of concept, we choose the simple pseudo-inverse method presented in Section 4.1 for the inverse kinematics.

In Figures 4a and 4b, we see that the USM is able to follow the desired end-effector velocity quite well. The observed error is mainly due to deviations in the control of the linear base frame velocity, observed in Figure 4c. Looking at Figures 4c, 4d, and 4e together, we see that the motion is indeed coordinated between the base frame and the manipulator joints. However, due to the particular choice of the pseudo-inverse method, no prioritization or control input preference is present. For this specific case study, this means that most of the motion is distributed to the base frame and the thrusters. This is also clearly visible from Figure 4f, where the linear motion of the end-effector and the base frame is compared.

7. CONCLUSIONS AND FUTURE RESEARCH

In this paper we have presented a control framework for underwater swimming manipulators and discussed the responsibilities of each subsystem in the framework. In particular, we have highlighted the challenge of controlling the velocity of the head link of the USM by coordinating the motion of the USM as a rigid body and the motion of the articulated joints. To solve the problem of motion coordination, we have investigated the applicability of inverse kinematic control of the USM. Furthermore, the interaction between the inverse kinematics routine and the thruster allocation algorithm have been explained. Finally, we have validated the proposed control framework through simulations by showing that the USM is able to achieve the desired end-effector velocity.

In future research, the authors will consider further development of each part of the proposed control framework in order to improve the performance and increase the robustness of the system.

REFERENCES

Antonelli, G. (2014). *Underwater Robots*. Springer International Publishing, 3rd edition.

Antonelli, G. and Chiaverini, S. (1998). Task-priority redundancy resolution for underwater vehicle-manipulator systems. In *Proc. IEEE International Conference on Robotics and Automation (ICRA)*, 768–773. Leuven, Belgium.

Antonelli, G. and Chiaverini, S. (2003). Fuzzy redundancy resolution and motion coordination for underwater vehicle-manipulator systems. *IEEE Trans. Fuzzy Syst.*, 11(1), 109–120.

Casalino, G., Zereik, E., Simetti, E., Torelli, S., Sperindé, A., and Turetta, A. (2012). Agility for underwater floating manipulation: Task & subsystem priority based control strategy. In *Proc. IEEE/RSJ International Conference on Intelligent Robots and Systems (IROS)*, 1772–1779. Vilamoura, Portugal.

Chiaverini, S. (1997). Singularity-robust task-priority redundancy resolution for real-time kinematic control of robot manipulators. *IEEE Transactions on Robotics and Automation*, 13(3), 398–410.

Egeland, O. (1987). Task-space tracking with redundant manipulators. *IEEE Journal on Robotics and Automation*, 3(5), 471 – 475.

Fossen, T. (1991). Adaptive macro-micro control of nonlinear underwater robotic systems. In *Proc. 5th International Conference on Advanced Robotics (ICAR)*, 1569–1572. Pisa, Italy.

From, P.J., Gravdahl, J.T., and Pettersen, K.Y. (2014). *Vehicle-Manipulator Systems: Modeling for Simulation, Analysis, and Control*. Advances in Industrial Control. Springer-Verlag.

Gilmour, B., Niccum, G., and O'Donnell, T. (2012). Field resident AUV systems - Chevron's long-term goal for AUV development. In *Proc. IEEE/OES Autonomous Underwater Vehicles (AUV)*, 1–5. Southampton, England.

Han, J., Park, J., and Chung, W.K. (2011). Robust coordinated motion control of an underwater vehicle-manipulator system with minimizing restoring moments. *Ocean Engineering*, 38(10), 1197–1206.

Johansen, T. and Fossen, T. (2013). Control allocation - A survey. *Automatica*, 49(5), 1087–1103.

Kelasidi, E., Pettersen, K.Y., Gravdahl, J.T., and Liljebäck, P. (2014). Modeling of underwater snake robots. In *Proc. IEEE International Conference on Robotics and Automation (ICRA)*, 4540–4547. Hong Kong, China.

Maciejewski, A. and Klein, C. (1985). Obstacle avoidance for kinematically redundant manipulators in dynamically varying environments. *International Journal of Robotics Research*, 4(3), 109–117.

Marani, G., Choi, S.K., and Yuh, J. (2009). Underwater autonomous manipulation for intervention missions AUVs. *Ocean Engineering*, 36(1), 15 – 23.

Matsuno, F. and Suenaga, K. (2003). Control of redundant 3D snake robot based on kinematic model. In *Proc. IEEE International Conference on Robotics and Automation (ICRA)*, 2061–2066. Taipei, Taiwan.

Mohan, S., Kim, J., and Kim, Y. (2012). A null space control of an underactuated underwater vehicle manipulator system under ocean currents. In *OCEANS 2012*, 1–5. IEEE, Yeosu.

Nakamura, Y., Hanafusa, H., and Yoshikawa, T. (1987). Task-priority based redundancy control of robot manipulators. *International Journal of Robotics Research*, 6(2), 3–15.

Pham, C. and From, P. (2013). Control allocation for mobile manipulators with on-board cameras. In *Proc. IEEE/RSJ International Conference on Intelligent Robots and Systems (IROS)*, 5002 – 5008. Tokyo, Japan.

Ridao, P., Carreras, M., Ribas, D., Sanz, P., and Oliver, G. (2014). Intervention AUVs: The Next Challenge. In *Proc. 19th IFAC World Congress (IFAC-WC)*, 12146–12159. Cape Town, South Africa.

Sarkar, N. and Podder, T.K. (2001). Coordinated motion planning and control of autonomous underwater vehicle-manipulator systems subject to drag optimization. *IEEE J.*

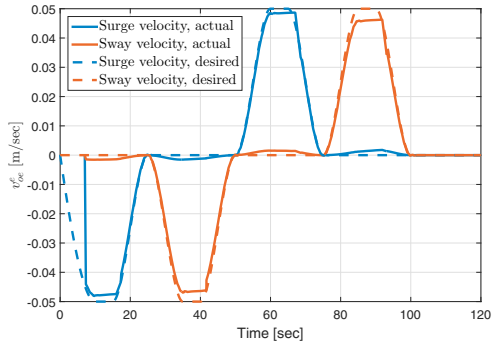

(a) End-effector linear velocities

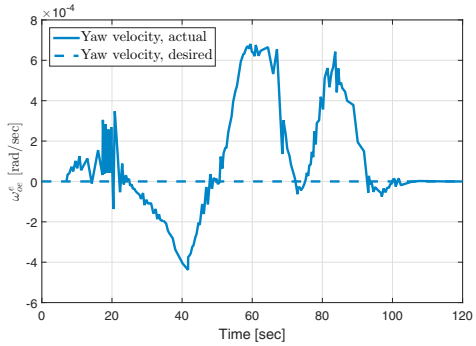

(b) End-effector angular velocity

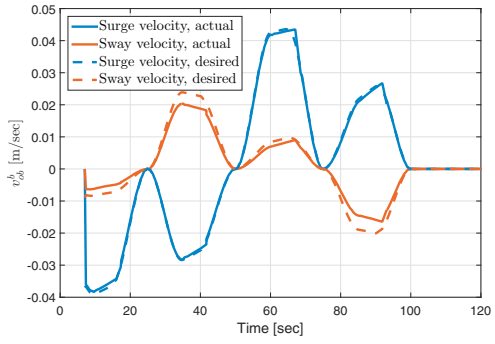

(c) Base frame linear velocities

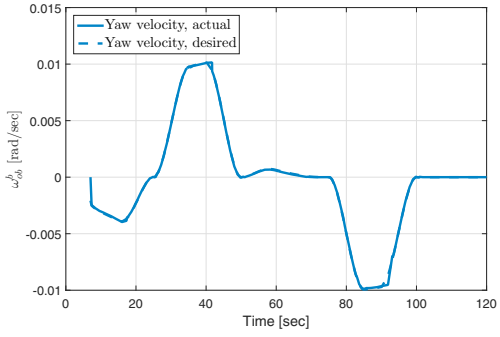

(d) Base frame angular velocity

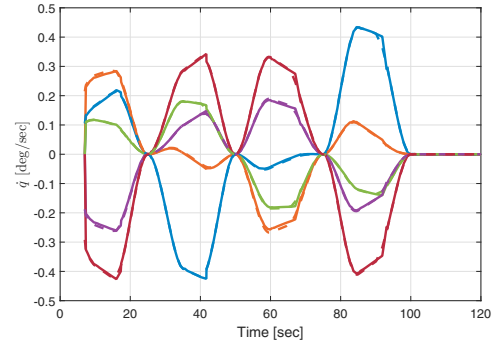

(e) Joint velocities

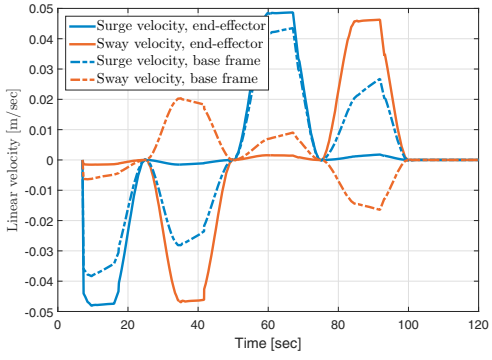

(f) End-effector and base frame velocities

Fig. 4. Simulation results for following a desired end-effector velocity

Oceanic Eng., 26(2), 228–239.

Sarkar, N., Yuh, J., and Podder, T.K. (1999). Adaptive control of underwater vehicle-manipulator systems subject to joint limits. In *Proc. IEEE/RSJ International Conference on Intelligent Robots and Systems (IROS)*, 142–147. Kyongju, South-Korea.

Schjølberg, I. and Fossen, T. (1994). Modelling and control of underwater vehicle-manipulator systems. In *Proc. 3rd Conf. on Marine Craft Maneuvering and Control (MCMC)*, 45–57. Southampton, UK.

Siciliano, B. and Slotine, J.J. (1991). A general framework for managing multiple tasks in highly redundant robotic systems. In *Proc. 5th International Conference on Advanced Robotics (ICAR)*, 12111216. Pisa, Italy.

Soylu, S., Buckham, B.J., and Podhorodeski, R.P. (2010). Redundancy resolution for underwater mobile manipulators. *Ocean Engineering*, 37(2-3), 325–343.

Sverdrup-Thygeson, J., Kelasidi, E., Pettersen, K.Y., and Gravdahl, J.T. (2016). Modeling of underwater swimming manipulators. In *Proc. 10th IFAC Conference on Control Applications in Marine Systems (CAMS)*. Trondheim, Norway.

Yamamoto, Y. and Yun, X. (1992). Coordinating locomotion and manipulation of a mobile manipulator. In *Proc. 31st IEEE Conference on Decision and Control (CDC)*, 2643–2648. Tucson, Arizona.